EFFECTS OF SUPPORT TYPE ON A 3-D CFD MODELLED HYDROGEN FED PLANAR SOFC

Mehmet T. Görüryılmaz, Muhittin Bilgili

Gazi University, Faculty of Engineering, Department of Mechanical Engineering, Maltepe 06570 Ankara
Corresponding author: Mehmet T. Görüryılmaz, e-mail: mtgoruryilmaz@gmail.com

REFERENCE NO	ABSTRACT
FCEL-05	Modelling is an important tool in the development of fuel cell systems. In this study, the numerical analysis of a Solid Oxide Fuel Cell (SOFC), having nickel/yttria stabilized zirconia (Ni/YSZ) cermet for anode side, strontium doped lanthanum manganite (LSM) for the cathode side and YSZ for the electrolyte, has been investigated for different thicknesses (support type) using CFD (Computational Fluid Dynamics) software FLUENT 15.0 code. The purpose is to see the effect of proposed component thickness on the performance of a single SOFC. Firstly, the developed model validated in agreement with the experimental data obtained from literature at the same conditions. Four different models have been developed; anode supported, cathode supported, electrolyte supported and non-supported. After obtaining the numerical results for each model, temperature, species, current density, pressure distributions and velocity profiles have been obtained and compared to each other.
Keywords: Solid oxide fuel cell, 3-Dimensional modelling, CFD, thickness, support type.	

1. INTRODUCTION

Solid oxide fuel cells (SOFCs) provide many advantages over traditional energy conversion systems including high efficiency, reliability, modularity, fuel adaptability, and very low levels of SOx and NOx emissions [1]. Electrical efficiency in SOFCs can reach values above 50% (even in small power ranges, which is the major advantage of FCs), due to its high working temperature, the SOFC can use hydrocarbons as fuel through an internal reforming process [2]. SOFCs operate at relatively high temperature, around 700 - 1000°C for maintaining high oxygen-ion-conductive of solid oxide electrolyte and such high temperature accelerates electrochemical reaction; therefore, they do not require precious metal catalysts to enhance the reaction [3]. The most commonly used anode cermet is nickel/yttria stabilized zirconia (Ni/YSZ); in techniques of the fabrication of NiO/YSZ anodes, this layer as fired is a dense material, and most of the porosity results from the reduction process while in most cases, the cathodes consist of perovskite materials like strontium doped lanthanum manganite (LSM) which is an efficient catalyst for the dissociation of oxygen molecules, and the electrolyte of an SOFC sandwiched between the anode and the cathode is a ceramic material that is impervious to gas transport and due to its excellent stability in both oxidizing and reducing atmospheres, YSZ is the most common electrolyte material [4]. As one of the common SOFC configurations, planar-type has attracted much more attention due to shorter current paths and higher power density over tubular-type design, to date, two main types planar SOFCs have been studied which are electrolyte- and electrode-supported designs; for electrolyte-supported SOFC, high working temperature is required in order to reduce the electrolyte ohmic loss, however, high working temperature is also a rigorous limit for materials of SOFC and decreases fuel cell lifetime and increases fabrication cost and for electrode-supported SOFC, electrolyte is very thin, which drastically reduces the electrolyte ohmic loss, thus electrode-supported SOFC can be operated at intermediate or low temperature and is preferred over electrolyte-supported design [5]. In the electrode-supported cell configuration, the electrolyte is usually very thin (i.e. 20 μm), and either the anode or the cathode is thick enough to serve as the supporting substrate for cell fabrication [6]. In the electrode-supported design, either the anode or the cathode is the thickest

component, however, cathode-supported SOFCs have a greater activation overpotential than anode-supported SOFCs, thus, the anode-supported SOFCs have received more attention in recent years [7]. Electrode support in an SOFC decreases the ohmic resistance and makes the design better suited for operation at lower temperatures (873-1073 K); the system is referred to as an 'intermediate-temperature solid oxide fuel cell' (IT-SOFC) and the development and performance improvement of an IT-SOFC have received much attention due to several potential benefits, e.g., the possibility of using a wider range of materials and the promise of low-cost fabrication; in an electrolyte-supported SOFC, the electrolyte is the thickest component (>150μm) while the anode and cathode are very thin, which results in high ohmic resistance, considering the characteristics of the electrode-supported SOFC, it has been reported that activation and concentration overpotentials can often outweigh the benefit of reduced ohmic loss due to smaller electrolyte thickness so that the specific resistance of the electrode-supported SOFC at an intermediate temperature may be larger than that of the high-temperature SOFC, further, it is well known that the performance characteristics of SOFCs are strongly affected not only by operating conditions such as temperature and pressure, and fuel and oxidant composition but also by structural parameters such as the thickness of electrodes and electrolyte and the porosity of electrodes, therefore, the performance analysis of fuel cells should take these parameters into account as it will lead to an optimum design and operation of SOFCs [8]. Understanding the details of the internal processes occurring within the SOFC experimentally is an expensive and challenging procedure [9]. The computer simulation technique has been used to investigate the cell performance in SOFCs [10]. Computer simulations of fuel cells involve complex multiphysics modeling, and earlier work on modeling these systems was faced with the challenge of unifying different solution procedures; the complexity of modeling is due to the fact that fuel cells are both multi-physics and multi-component systems [11]. Numerical methods, such as the finite element or finite volume method, enable modelling complicated geometry in a relatively short time while providing a solution sufficiently accurate for engineering purposes and the numerical approaches of computational fluid dynamics (CFD) have, in most cases, proven to be a powerful tool to aid in reduced physical prototype costs and product development time [12]. For validating the SOFC models, we need to consider in-situ measurable major properties, such as voltage, current, and temperature and among these properties, I-V (current-voltage) validation and temperature validation seem to be the most practical options, which together are to provide insights on concentration variations [13].

The modelling of an SOFC consists the following parts; current collectors, anode, cathode and a solid ceramic electrolyte. The porous medias, which are the anode and the cathode, are the layers which electrochemical reactions take place. The anode is usually nickel/yttria stabilized zirconia (Ni/YSZ) cermet and the cathode is strontium doped lanthanum manganite (LSM). These electrode layers are separated by an electrolyte, which is usually YSZ.

The aim of this study is to investigate the differences, which are temperature, current density, species, fuel utilizations, pressure and velocities, caused by support type in SOFCs by using CFD method, using ANSYS FLUENT Fuel Cells Module. This study concerns of gathering different possibilities of support types in one paper. While there are studies that compares anode- to cathode-supported models [5] or anode- to electrolyte-supported models [16], there is a lack of studies on focusing of comparing all at once. Hence, this paper aims to enhance and contribute to the field by observing the effects of different support types of SOFC.

2. MODEL GEOMETRY

SOFCs require high temperatures. Thus, setting up an experiment is difficult, costly and time consuming. Because of this reason,

CFD methods are popular in this field. The experimental setup based in this study can be found in [14]. A numerical model was prepared based on the experiment, the obtained results using numerical method have been compared with experimental data from the literature. Based on this model, three more geometries have been modelled (cathode supported, electrolyte supported and non-supported) to observe the effect of the component thickness. Values of the anode supported geometry can be found in Table 1.

Table 1: Geometry dimensions and values for the anode supported model

Part Name	Length
Cell Length	40 mm
Cell Width	20 mm
Channel Height	1 mm
Channel Width	2 mm
Number of Channels	6.5
Current Collector Thickness	1.3 mm
Cathode Diffusion Layer Thickness	0.05 mm
Cathode/Anode Active Layer Thickness	0.02 mm
Electrolyte Layer Thickness	0.01 mm
Anode Diffusion Layer Thickness	0.38 mm

For the cathode supported geometry, the thickness of the cathode diffusion layer was set to 0.38 mm and the anode diffusion layer thickness was set to 0.05 mm and the rest of values of dimensions kept fixed. For the electrolyte supported model, the electrolyte thickness was set to 0.38 mm while the anode and the cathode diffusion layer thicknesses were set to 0.05 mm and the rest of the values kept fixed as well. Finally, for the non-supported geometry, the anode diffusion layer thickness was set to 0.05 mm while the rest of the values kept fixed. The mesh structures have been compiled via ICEM-CFD with all of the cells 95-100% quality quadrilateral meshes and after several different mesh numbers, the mesh independence achieved between 900 000 – 1 000 000 meshes.

The results have been obtained via CFD code FLUENT. In this study, four kinds of boundary conditions have been used. Firstly, wall boundary condition is used to separate the solids and fluids. The top and the bottom walls of the cell are different from the other walls since the external circuit connected to these surfaces. The potential of the anode terminal wall is set to zero and the cathode terminal wall is set to operating cell voltage. Then mass flow inlets have been applied to the inlets and pressure outlets have been applied to the outlets for 1 atm. Finally, a symmetry boundary condition has been used to reduce the solving time.

3. MODELING EQUATIONS AND PARAMETERS

Finite volumes method has been used to solve the fuel cell equations. For steady-state mass conservation;

$$\frac{\partial(\varepsilon\rho u)}{\partial x} + \frac{\partial(\varepsilon\rho v)}{\partial y} + \frac{\partial(\varepsilon\rho w)}{\partial z} = S_m \qquad (1)$$

equation has been defined. In this equation, u, v and w are the velocities of x, y and z directions, respectively while ρ is density, ε porosity and S_m is the source term. The values of porosity changes from layer to layer according to layer qualities and in the non-porous layers, such as flow channels and current collectors, this value is 1.
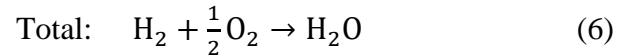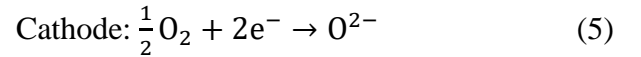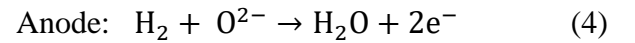
For the momentum conservation;

$$\frac{\partial}{\partial t}(\rho\,v) + \nabla.(\rho\,v\,v) = -\nabla p + \nabla(\tau) + \rho g + F \quad (2)$$

For an incompressible flow, energy conversation equation is;

$$\frac{\partial}{\partial t}(\rho E) + \nabla.[v(\rho E + p)] = \nabla[k_{eff}\nabla T - \sum_j h_j J_j + (\tau_{eff}.v)] + S_h \qquad (3)$$

S_h is the volumetric source or the sink of energy and should be added to ohmic heat energy equation in all electrical conductive regions. In a hydrogen fed SOFC, the chemical reactions are as follows;

Anode: $H_2 + O^{2-} \rightarrow H_2O + 2e^- \qquad (4)$

Cathode: $\frac{1}{2}O_2 + 2e^- \rightarrow O^{2-} \qquad (5)$

Total: $H_2 + \frac{1}{2}O_2 \rightarrow H_2O \qquad (6)$

The open circuit voltage (OCV) is locally calculated with gas composition and temperature in the electrodes, which can be determined by the Nernst equation;

$$OCV = E^0 - \frac{RT}{2F}\ln\left(\frac{P_{H_2O}}{P_{H_2}\sqrt{P_{O_2}}}\right) \qquad (7)$$

In Eq. (7), R is gas constant, T is Temperature, F is Faraday constant and P_{H_2O}, P_{H_2}, P_{O_2} are the partial pressures of steam, hydrogen and oxygen, respectively. E^0 is the potential for the hydrogen oxidation reaction at the standard temperature and pressure, which is the change in Gibbs free energy, ΔG;

$$E^0 = \frac{\Delta G}{2F} \qquad (8)$$

The OCV is the maximum potential a fuel cell can reach. The actual voltage of a cell is the potential difference between anode and cathode. And this value is always lower than the OCV. Various potential losses affect the difference between OCV and cell voltage E. These losses are the ohmic, activation and concentration losses.

$$E = OCV - \eta_{act} - \eta_{conc} - I \times R_{ohm} \qquad (9)$$

In this equation, η_{act} indicates the activation losses, η_{conc} indicates concentration losses, I indicates the local current density. The concentration losses occur due to slow supply of the reactants for the reaction. This happens at the high current densities when the reaction rate is high. The activation losses occur because of the slow rates of the reactions at the active layers.

The volumetric current densities in an SOFC can be calculated by using Butler-Volmer equation.

$$R_{an} = \left(\zeta_{an} i_{an}^{ref}\right)\left(\frac{[A]}{[A]_{ref}}\right)^{\gamma_{an}} \left(e^{\alpha_{an}F\eta_{an}/RT} - e^{-\alpha_{cat}F\eta_{an}/RT}\right) \qquad (10)$$

$$R_{cat} = \left(\zeta_{cat} i_{cat}^{ref}\right)\left(\frac{[C]}{[C]_{ref}}\right)^{\gamma_{cat}} \left(-e^{\alpha_{an}F\eta_{cat}/RT} + e^{-\alpha_{cat}F\eta_{cat}/RT}\right) \qquad (11)$$

Here, i^{ref} is the reference exchange current density per active area, ζ is specific active surface area, $[\,]$, $[\,]_{ref}$ are the local concentrations of species corresponding to their zones, γ is concentration dependence, α transfer coefficient and F is Faraday constant. i^{ref} can be expressed as;

$$i^{ref} = \frac{RT}{nF} A_i e^{-E_a/RT} \qquad (12)$$

This value of i^{ref} can be used as a calibration parameter of the model. In this study, reference exchange current density was fitted to calibrate the model results [17].

While majority of the electrons are transported in the anode and the cathode, the majority of the ions are transported in the electrolyte. The ions are produced at the TPBs (Triple Phase Boundary) at the cathode by oxygen atoms and these ions are transferred to the TPB of the anode side through the electrolyte and consumed there by reacting with the hydrogen atoms. The electronic conductivities of the TPB electrodes and the ionic conductivity of the electrolyte can be expressed as;

$$\sigma_{electron,a} = \frac{4.2 \times 10^7}{T} e^{\frac{-1200}{T}} \qquad (13)$$

$$\sigma_{electron,c} = \frac{9.5 \times 10^7}{T} e^{\frac{-1150}{T}} \qquad (14)$$

$$\sigma_{ion,elect} = \frac{3.34 \times 10^4}{T} e^{\frac{-10\,300}{T}} \qquad (15)$$

The effective conductivity for the porous electrodes is;

$$\sigma_{eff} = \left(\frac{1-\varepsilon}{\tau}\right) \times \sigma \times V_{eff} \qquad (16)$$

Here, ε is the porosity of the porous electrodes, τ is the tortuosity, factor of charge transport and the V_{eff} is the volume fraction of Ni or LSM corresponding to their electrodes. The values of these parameters are given in Table 2 and the other values can be seen in Table 3. It has been found that the current collectors are stainless steels [15]. The conductivity of the current collectors has been determined by comparing [20] and FLUENT Fuel Cells Module database. After the comparison, FLUENT value has been used.

Table 2: Charge transport properties

	ε	τ	V_{eff}
Anode	0.3	10	YSZ/Ni : 0.6/0.4
Cathode	0.3	10	YSZ/LSM: 0.6/0.4

Table 3: Material properties

	Anode Diffusion Layer	Anode Active Layer (TPB)	Electrolyte	Cathode Active Layer (TPB)	Cathode Diffusion Layer	Current Collectors (Interconnectors)
Porosity	0.35	0.3	0	0.3	0.35	0
Pearmability (m^2)	2e-10	2e-11	0	2e-11	2e-10	0
Tortuosity	10	10	-	10	10	-
Specific Heat (J/kgK)	450	450	550	430	430	550
Thermal Conductivity (W/mK)	11	11	2.7	6	6	20
Specific Area (1/m)	1.08e+05	1.03e+05	-	2.6e+06	1.08e+05	-

4. RESULTS AND DISCUSSION

In order to investigate the support types of SOFCs, four different models were designed. As seen on Fig. 1, the polarization curve results of the anode supported model is in a good agreement with the experimental results of Zhang et al. [14] in the literature.
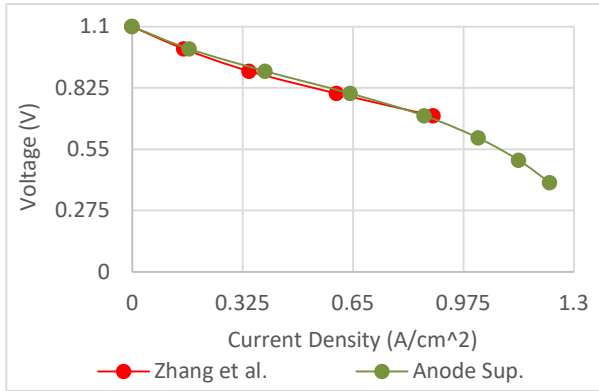
Fig. 1: Polarization Curve of Anode Supported Experiment and Model

After obtaining the curve on Fig. 1, the other geometries have been solved numerically and polarization curves have been obtained. Fig. 2 shows the comparison of the polarization curves for four different support types (anode supported, cathode supported, electrolyte supported and non-supported).
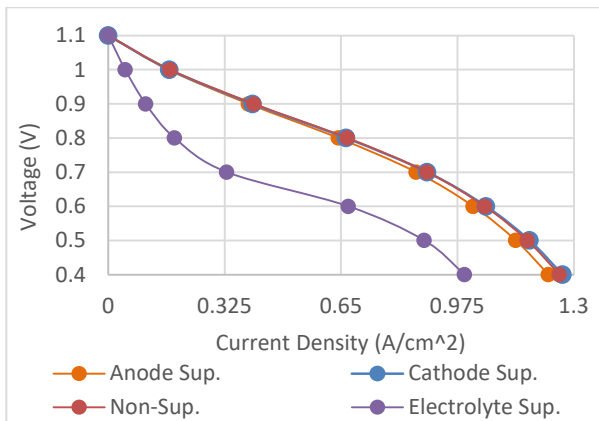

Fig. 2: Polarization Curves of the Models

From the Fig. 2, it is seen that the difference between the current densities of the anode-, the cathode- and the non-supported models are small compared to the electrolyte supported model. While the electrolyte supported model has the lowest value, the cathode supported model has the highest value. The dramatic decrease of the current density in the electrolyte supported model is mostly caused by the ohmic losses. For 0.7 V of operating voltage, the non-supported model has a higher current density value by 3.42% than the anode supported model and the cathode supported model has a higher value by 0.02% than the non-supported model. The difference between the electrolyte and the anode supported model is 61.46%, the current density of the anode supported model is higher.

The numbers given to the models in the graphics at the end of the figures 4, 5 and 6 are as follows; 1 is the anode supported, 2 is the cathode supported, 3 is non-supported and 4 is the electrolyte supported SOFCs. The results have been taken for the operating voltage of 0.7 V.

Figure 3 shows the difference between temperatures. As seen on the figure, the non-supported model has the highest temperature where the electrolyte supported model has the lowest. And the other models in between, the anode supported model has lower temperature than the cathode supported model. This situation satisfies the Fig. 2 given above. It is observed that lower the layer thicknesses causes higher temperatures. Hence, it can be said that it is easier for the electrochemical reactions to occur with thinner layers. The reason of the low current density on the

electrolyte supported cell is that the thicker the layer, less and longer the electron transfer which results in a loss. These results also agree with the current densities and fuel utilizations.
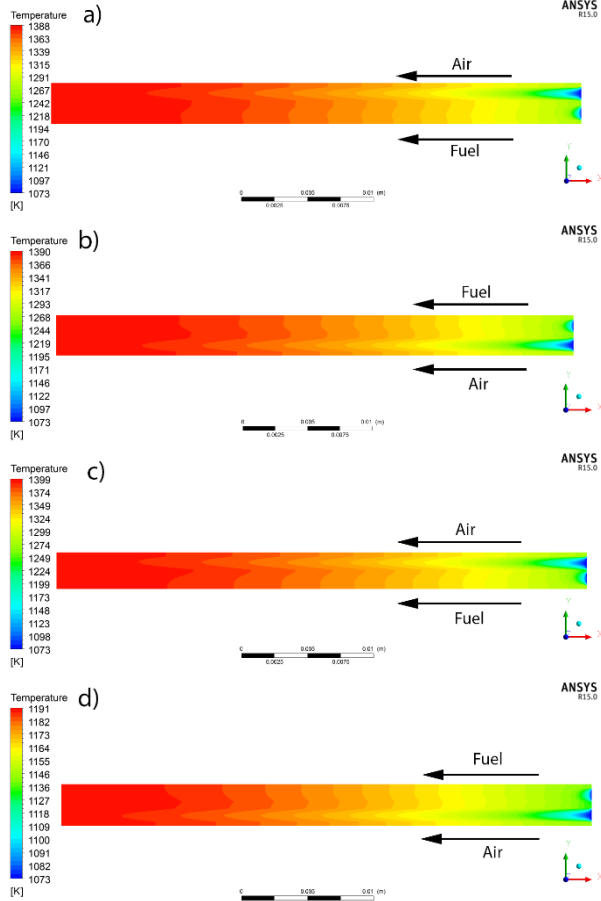

Fig. 3: Temperatures of the models, symmetry planes
a) Anode supported, b) Cathode Supported,
c) Non-supported, d) Electrolyte Supported

Fig. 4 represents the difference between the maximum current densities at the operating voltage of 0.7 V. As seen on Fig. 4, the non-supported model has the highest current density compared to others. The cathode supported model, the anode supported model and the electrolyte supported model follow the non-supported model respectively. The contours have been scaled for a better visual, real maximum values can be seen on the graphic.
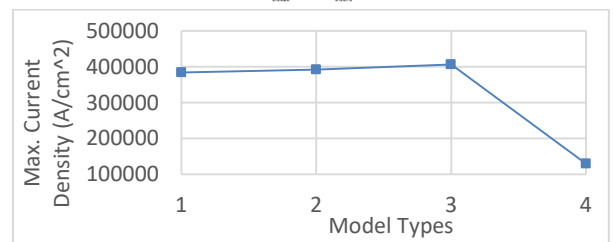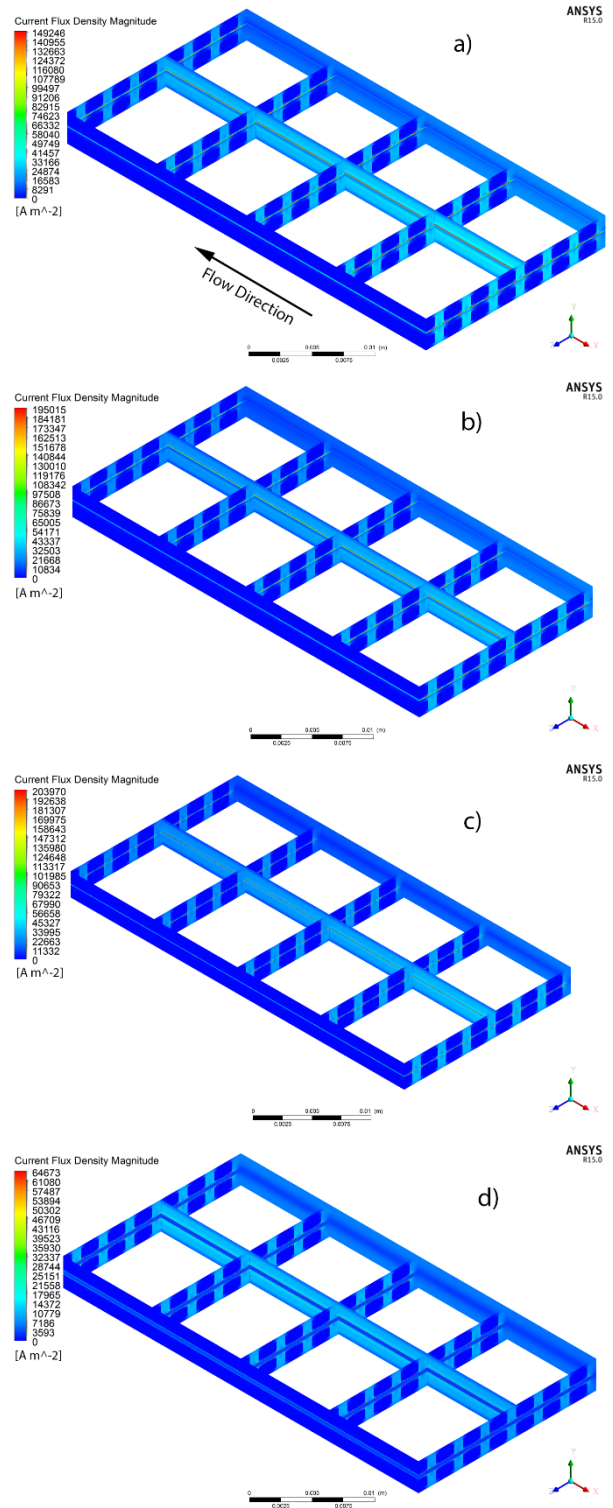
Fig. 4: Current densities of the models
a) Anode supported, b) Cathode Supported,
c) Non-supported, d) Electrolyte Supported

In Fig. 5, it can be seen that the highest fuel utilization belongs to the non-supported model. This indicates that the electrochemical reactions occur in non-supported models more than the others, as said before for temperature. Because the thinner layers make electron transfer easier and enhances the diffusion.
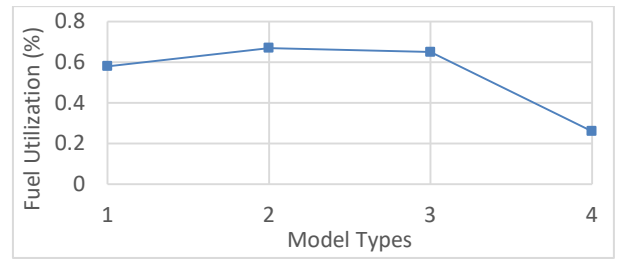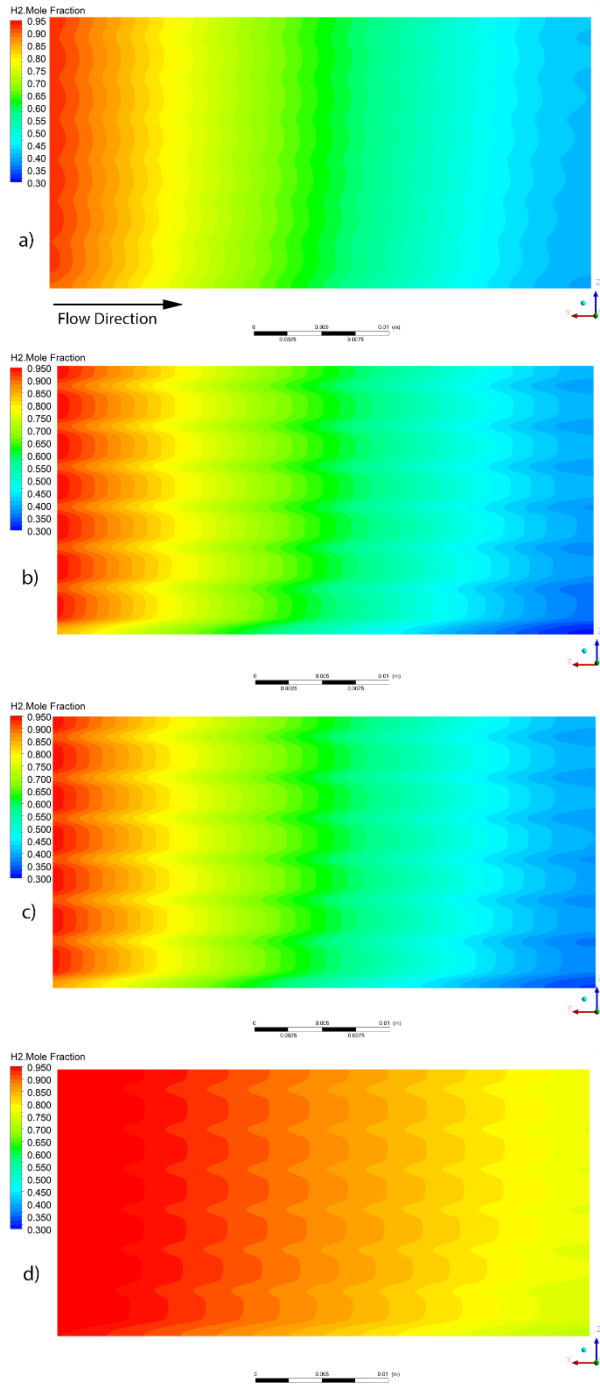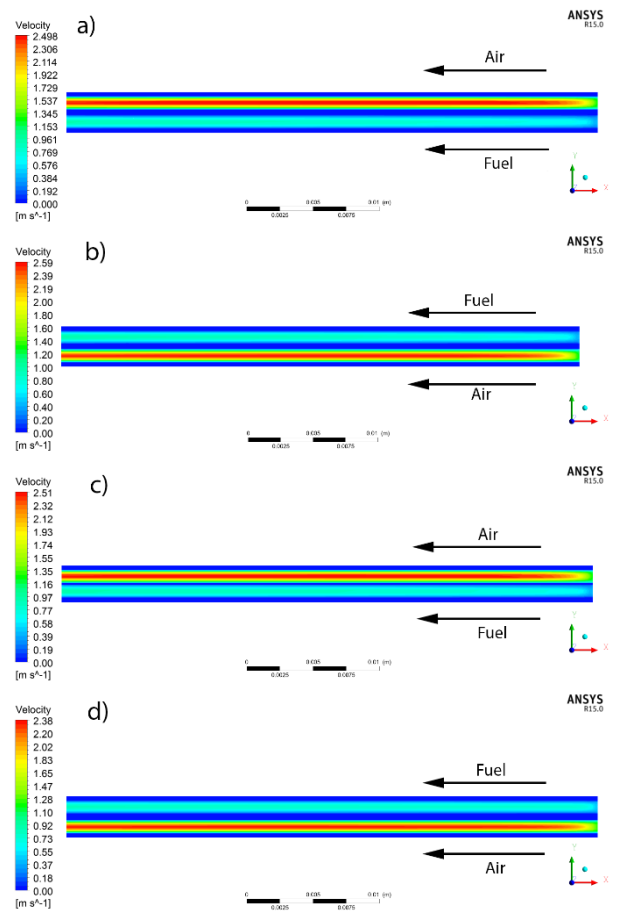

Fig. 5: Hydrogen distributions of the models, middle planes of the anodic active areas
a) Anode supported, b) Cathode Supported,
c) Non-supported, d) Electrolyte Supported

Fig. 6 shows the velocity distributions of the models, taken from the symmetry planes. For each model, it is seen that the velocity of the air channels is higher than the fuel channels, which is in an agreement with the inlet flow rates of the gases. For all the models, the velocities of the gases increase along with the flow and reach the highest value at the outlets. This situation is in an agreement with the temperature increase and fuel utilizations.
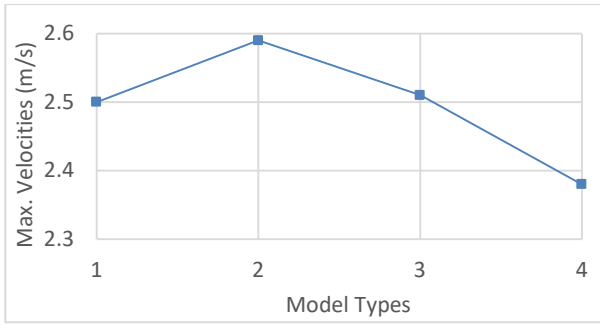
Fig. 6: Velocities of the models, symmetry planes
a) Anode supported, b) Cathode Supported,
c) Non-supported, d) Electrolyte Supported

The distributions of the hydrogen mole fractions can be seen in Fig. 7. As seen in the figures, the distribution follows and elliptic shape from top to the bottom of the channel. The reason is that the electrochemical reactions occur close to the electrolyte surface and as the hydrogen gets closer to the surface, it will join the reactions, hence the percentage will drop closer to the electrolyte surface.
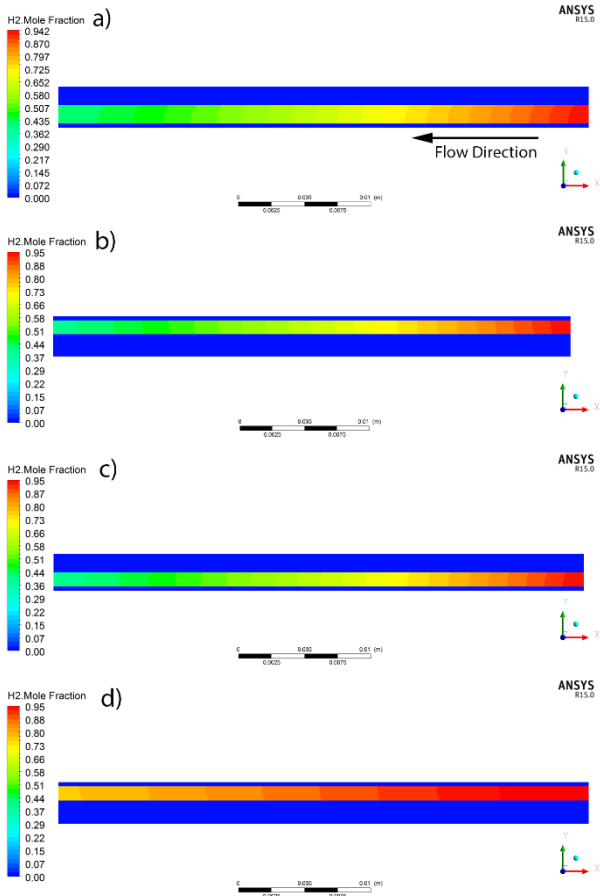

Fig. 7: Hydrogen distributions, symmetry planes
a) Anode supported, b) Cathode Supported,
c) Non-supported, d) Electrolyte Supported

Fig. 8 shows the oxygen distribution along the symmetry plane. Since the velocity of the gas is higher at the cathode side, it is observed that the decrease in the y-axis is more uneven compared to the hydrogen distribution. Even though the contour lines look like the hydrogen distribution (in manners of ellipticity and decreasing way), it can be clearly seen that the diffusion of oxygen is slower than the hydrogen.
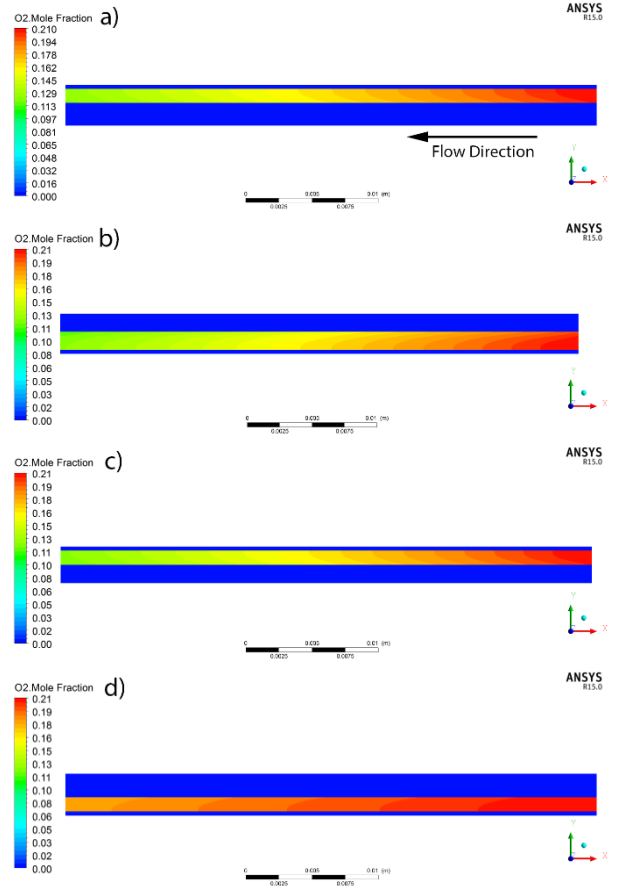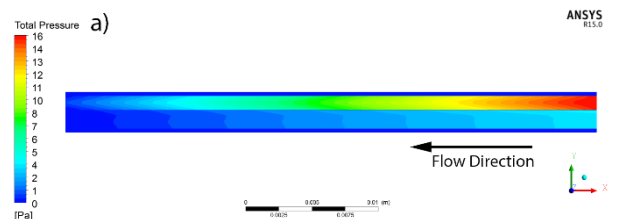

Fig. 8: Oxygen distributions, symmetry planes
a) Anode supported, b) Cathode Supported,
c) Non-supported, d) Electrolyte Supported

Fig. 9 shows the pressure distributions on symmetry planes. As seen in the figure, the higher flow rates (thus higher velocities, which are the cathode sides) have higher pressures. Pressure drop in anode sides are less compared to cathode sides. Fig. 9 also shows that the pressure drop comparison between the models are almost the same.
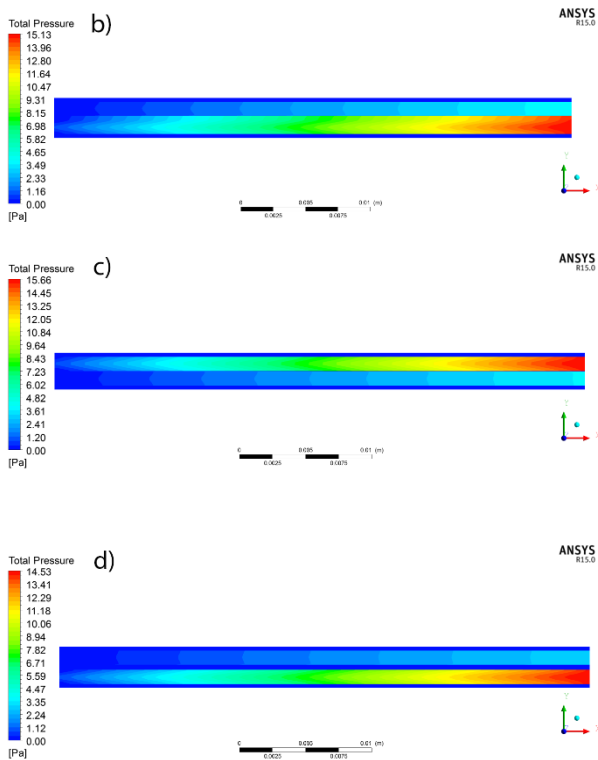
Fig. 9: Total pressure distributions, symmetry planes
a) Anode supported, b) Cathode Supported,
c) Non-supported, d) Electrolyte Supported

5. CONCLUSION

In this study, four different geometries have been analysed numerically and the results have been discussed for a hydrogen fed planar SOFC. The anode supported model is in a very well agreement with the experiment. Thus, it can be accepted that the other developed models will be in a good agreement with actual cells. Polarization curves, temperature distributions, current density distributions, fuel utilizations, velocities, pressures and species distributions have been presented and discussed.

It is seen that the support type has an immense effect on the cell. Depending on the support type, cells have different efficiencies and feasibility effects, but this does not mean that the higher fuel utilization and current density values lead to a better cell. Further investigations for mechanical properties (i.e. stresses) should be done and compared to one another. Because of the high temperatures, cracks may occur in the components and this causes the cell to stop working, which is not desirable. Consequently, different support types (i.e. cathode supported cell) may

provide better outputs for SOFCs in manner of current density and fuel utilization.

Nomenclature

E^0 Hydrogen oxidation reaction potential (V)
F   Faraday constant (C/mol)
G   Gibbs free energy (kJ/mol)
I   Local current density (A/m^2)
P_X Partial pressure of relevant gas of X
OCV   Open circuit voltage (V)
R   Gas constant (kJ/kmolK)
R_{ohm} Ohmic resistance
S_m Source term
S_h Volumetric source/sink of energy
T   Temperature (K)

Greek Letters

α Transfer Coefficient
γ Concentration Dependence
ε Porosity
ζ Specific Active Surface Area
η Losses
ρ Density
σ Conductivity
τ Tortuosity

References

[1] Pern S, Chen C, Numerical Investigation of Anode Thickness on the Performance and Heat/Mass Transport Phenomenon for an Anode-Supported SOFC Button Cell, Journal of Nanomaterials, 2015, 2015

[2] Razbani O, Assadi M, Anderson M, Three Dimensional CFD Modeling And Experimental Validation of an Electrolyte Supported Solid Oxide Fuel Cell Fed with Methane-Free Biogas, International Journal of Hydrogen Energy, 2013, 38, 10068-10080

[3] Wang Y, Yoshiba F, Watanabe T, Weng S, Numerical Analysis of Electrochemical Characteristics and Heat/Species Transport for Planar Porous-Electrode-Supported SOFC, Journal of Power Sources, 2007, 170, 101-110

[4] Deutschmann O, Janardhanan V.M, Modeling of Solid-Oxide Fuel Cells, Zeitschrift für Physikalische Chemie, 2007, 221, 443-478

[5] Su S., Gao X., Zhang Q., Kong W., Chen D., Anode- Versus Cathode-Supported Solid Oxide Fuel Cell: Effect of Cell Design on the

Stack Performance, International Journal of Electrochemical Science, 2015, 10, 2487-2503

[6] Das R, Reddy R, Computational Modeling of a Planar 3-D SOFC and the Effect of Materials Properties on the Anode Performance, Journal for Manufacturing Science and Production, 2009, 10, 43-52

[7] Wang W, Yang S, Chen T, Wang Y, Peng Z, Electrochemical Analysis of an Anode-Supported SOFC, International Journal of Electrochemical Science, 2013, 8, 2330 - 2344

[8] Arpornwichanop A, Chuachuensuk A, Patcharavorachot Y, Electrochemical Study of a Planar Solid Oxide Fuel Cell: Role of Support Structures, Journal of Power Sources, 2008, 177, 254-261

[9] Wei S.-S, Wang T.-H, Wu J.-S, Numerical Modeling of Interconnect Flow Channel Design and Thermal Stress Analysis of a Planar Anode-Supported Solid Oxide Fuel Cell Stack, Energy, 2014, 69, 553-561

[10] Yakabe H, Ogiwara T, Hishinuma M, Yasuda I, 3-D Model Calculation for Planar SOFC, Journal of Power Sources, 2001, 102, 144-154

[11] Smirnov A, Burt A, Celik I, Multi-Physics Simulations of Fuel Cells Using Multi-Component Modeling, Journal of Power Sources, 2006, 158, 295-302

[12] Peksen M, Peters R, Blum L, Stolten D, Numerical Modelling and Experimental Validation of a Planar Type Pre-Reformer in SOFC Technology, International Journal of Hydrogen Energy, 2009, 34, 6425-6436

[13] Aydın Ö, Nakajima H, Kitahara T, Reliability of the Numerical SOFC Models for Estimating the Spatial Current and Temperature Variations, International Journal of Hydrogen Energy, 2016, 41, 15311-15324

[14] Zhang Z, Yue D, He C, Ye S, Wang W, Yuan J, Three-Dimensional CFD Modeling Of Transport Phenomena in Anode-Supported Planar SOFCs, Heat and Mass Transfer, 2014, 50, 1575-1586

[15] Andersson M, Yuan J, Sunden B, SOFC Modeling Considering Electrochemical Reactions at The Active Three Phase Boundaries, International Journal of Heat and Mass Transfer, 2012, 55, 773-788

[16] Droushiotis N., Dal Grande F., Dzarfan Othman M. H., Kanawka K., Doraswami U., Metcalfe I. S., Li K., Kelsall G., Comparison Between Anode-Supported and Electrolyte-Supported Ni-CGO-LSCF Micro-tubular Solid Oxide Fuel Cells, Fuel Cells From Fundamentals To Systems, 2014, 14, 200-211

[17] Iranzo A, Muñoz M, Rosa F, Pino J, Numerical Model for The Performance Prediction of A PEM Fuel Cell. Model Results and Experimental Validation, International Journal of Hydrogen Energy, 2010, 35, 11533-11550

[18] Milewski J, Swirski K, Santarelli M, Leone P, Advanced Methods of Solid Oxide Fuel Cell Modeling, Springer, 2011

[19] Taroco H. A., Santos J. A. F., Domingues R. Z., Matencio T., Ceramic Materials for Solid Oxide Fuel Cells, Advances in Ceramics - Synthesis and Characterization, Processing and Specific Applications, 2011, InTech

[20] Yang Z.G., Stevenson J.W., Paxton D.M., Singh P, Weil K.S., Materials Properties Database for Selection of High-Temperature Alloys and Concepts of Alloy Design for SOFC Applications, 2002, United States Department of Energy

[21] 15.0, ANSYS FLUENT, Fuel Cells Module Manual

[22] 15.0, ANSYS ICEM-CFD, User Manual